

## Seasonal variability of GPS-derived zenith tropospheric delay (1994–2006) and climate implications

Shuanggen Jin,<sup>1,2</sup> Jong-Uk Park,<sup>1</sup> Jung-Ho Cho,<sup>1</sup> and Pil-Ho Park<sup>1</sup>

Received 10 July 2006; revised 21 November 2006; accepted 14 December 2006; published 8 May 2007.

[1] The total zenith tropospheric delay (ZTD) is an important parameter of the atmosphere and directly or indirectly reflects the weather and climate processes and variations. In this paper the ZTD time series with a 2-hour resolution are derived from globally distributed 150 International GPS Service (IGS) stations (1994–2006), which are used to investigate the secular trend and seasonal variation of ZTD as well as its implications in climate. The mean secular ZTD variation trend is about  $1.5 \pm 0.001$  mm/yr at all IGS stations. The secular variations are systematically increasing in most parts of the Northern Hemisphere and decreasing in most parts of the Southern Hemisphere. Furthermore, the ZTD trends are almost symmetrically decreasing with increasing altitude, while the summation of upward and downward trends at globally distributed GPS sites is almost zero, possibly reflecting that the secular ZTD variation is in balance at a global scale. Significant annual variations of ZTD are found over all GPS stations with the amplitude from 25 to 75 mm. The annual variation amplitudes of ZTD near oceanic coasts are generally larger than in the continental inland. Larger amplitudes of annual ZTD variation are mostly found at middle latitudes (near 20°S and 40°N) and smaller amplitudes of annual ZTD variation are located at higher latitudes (e.g., Antarctic) and the equator areas. The phase of annual ZTD variation is about 60° in the Southern Hemisphere (about February, summer) and about 240° in the Northern Hemisphere (about August, summer). The mean amplitude of semiannual ZTD variations is about 10 mm, much smaller than annual variations. The semiannual amplitudes are larger in the Northern Hemisphere than in the Southern Hemisphere, indicating that the semiannual variation amplitudes of ZTD in the Southern Hemisphere are not significant. In addition, the higher-frequency variability (RMS of ZTD residuals) ranges from 15 to 65 mm of delay, depending on altitude of the station. Inland stations tend to have lower variability and sites at ocean and coasts have higher variability. These seasonal ZTD cycles are due mainly to the wet component variations (ZWD).

**Citation:** Jin, S., J.-U. Park, J.-H. Cho, and P.-H. Park (2007), Seasonal variability of GPS-derived zenith tropospheric delay (1994–2006) and climate implications, *J. Geophys. Res.*, 112, D09110, doi:10.1029/2006JD007772.

### 1. Introduction

[2] The GPS signal is delayed by the neutral atmosphere, which results in lengthening of the geometric path of the ray, usually referred to as the “tropospheric delay.” This delay is one of major error sources for GPS positioning, which contributes a bias in height of several centimeters even when simultaneously recorded meteorological data are used in tropospheric models [Fang *et al.*, 1998; Tregoning *et al.*, 1998]. Nowadays, GPS has been widely used to determine the zenith tropospheric delay (ZTD) [Ewardson *et al.*, 1998; Vedel *et al.*, 2001; Jin and Park, 2005] through mapping functions [Niell, 1996]. The ZTD is the integrated

refractivity along a vertical path through the neutral atmosphere:

$$ZTD = c\tau = 10^{-6} \int_0^{\infty} N(s) ds \quad (1)$$

where  $c$  is the speed of light in a vacuum,  $\tau$  is the delay measured in units of time, and  $N$  is the neutral atmospheric refractivity. The  $N$  is empirically related to standard meteorological variables as [Davis *et al.*, 1985]

$$N = k_1 \rho + k_2 \frac{P_w}{Z_w T} + k_3 \frac{P_w}{Z_w T^2} \quad (2)$$

where  $k_i$  ( $i = 1, 2, 3$ ) is constant,  $\rho$  is the total mass density of the atmosphere,  $P_w$  is the partial pressure of water vapor,  $Z_w$  is a compressibility factor near unity accounting for the small departures of moist air from an ideal gas, and  $T$  is the temperature in degrees Kelvin. The integral of the first term of equation (2) is the hydrostatic component ( $N_h$ ) and the

<sup>1</sup>Space Geodesy Division, Korea Astronomy and Space Science Institute, Daejeon, South Korea.

<sup>2</sup>Also at Shanghai Astronomical Observatory, Chinese Academy of Sciences, Shanghai, China.

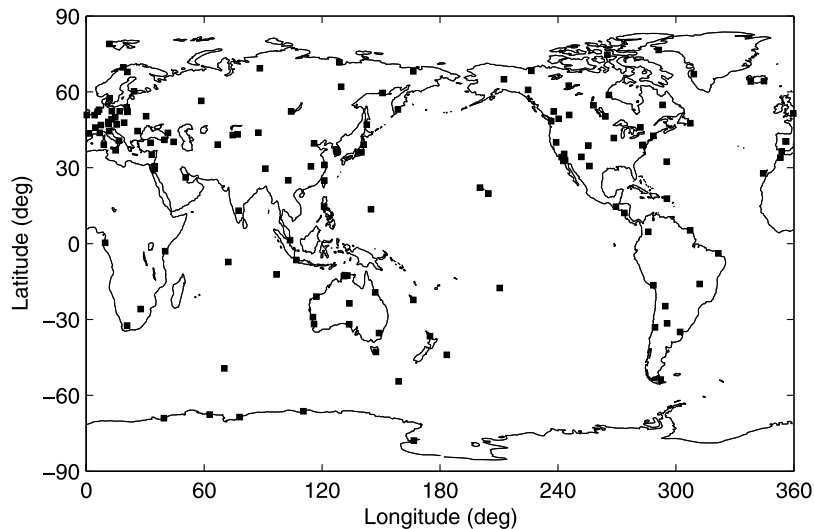


**Figure 1.** Distribution of global International GPS Service (IGS) GPS sites.

integral of the remaining two terms is the wet component ( $N_w$ ). Thus ZTD is the sum of the hydrostatic or “dry” delay (ZHD) and nonhydrostatic or “wet” delay (ZWD), due to the effects of dry gases and water vapor, respectively. The dry component ZHD is related to the atmospheric pressure at the surface, while the wet component ZWD can be transformed into the precipitable water vapor (PWV) and plays an important role in energy transfer and in the formation of clouds via latent heat, thereby directly or indirectly influencing numerical weather prediction (NWP) model variables [Bevis et al., 1994; Duan et al., 1996; Tregoning et al., 1998; Manuel et al., 2001]. Therefore the Zenith Tropospheric Delay (ZTD) is an important parameter of the atmosphere, which reflects the weather and climate processes, variations, and atmospheric vertical motions, etc.

[3] In the last decade, ground-based GPS receivers have been developed as all-weather, high spatial-temporal resolution and low-cost remote sensing systems of the atmosphere [Bevis et al., 1994; Manuel et al., 2001], as compared to conventional techniques such as satellite radiometer sounding, ground-based microwave radiometer, and radiosondes [Westwater, 1993]. With independent data from other instruments, in particular water vapor radiometers, it has been demonstrated that the total zenith tropospheric delay or integrated water vapor can be retrieved using ground-based GPS observations with the same level of accuracy as radiosondes and microwave radiometers [Elgered et al., 1997; Bevis et al., 1992; Rocken et al., 1993; Duan et al., 1996; Emaradson et al., 1998; Fang et al., 1998; Tregoning et al., 1998]. Currently, the International GPS Service (IGS) has operated a global dual frequency GPS receiver observation network with more than 350 permanent GPS sites since 1994 [Beutler et al., 1999]. It provides a high and wide range of scales in space and time to study on seasonal and secular

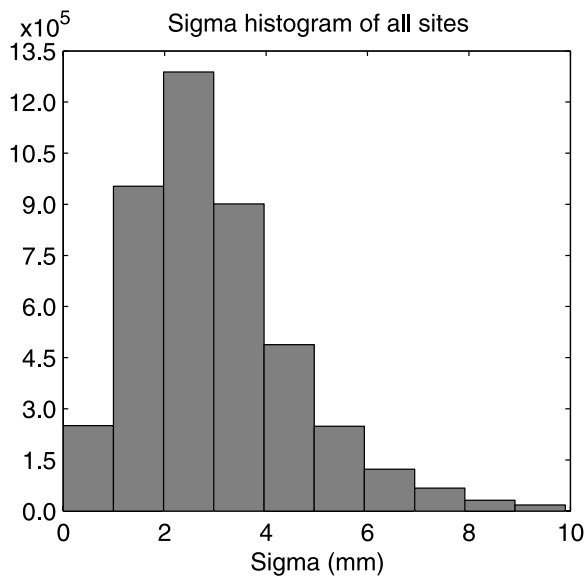


**Figure 2.** Histogram of the uncertainty for the zenith tropospheric delay (ZTD) solutions at 150 sites.

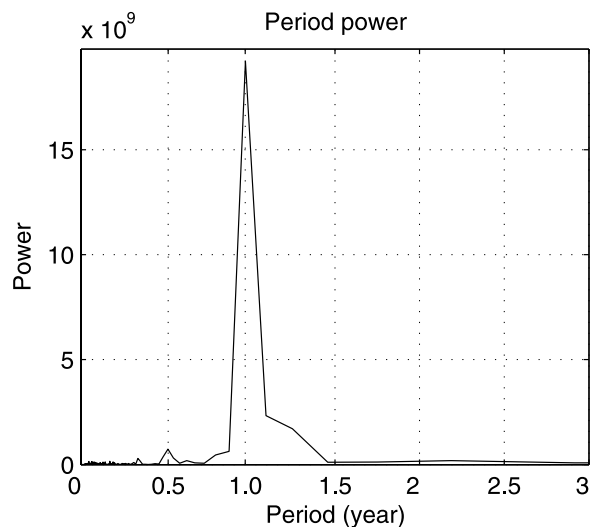


**Figure 3.** Power chart of ZTD time series at Wuhan site.

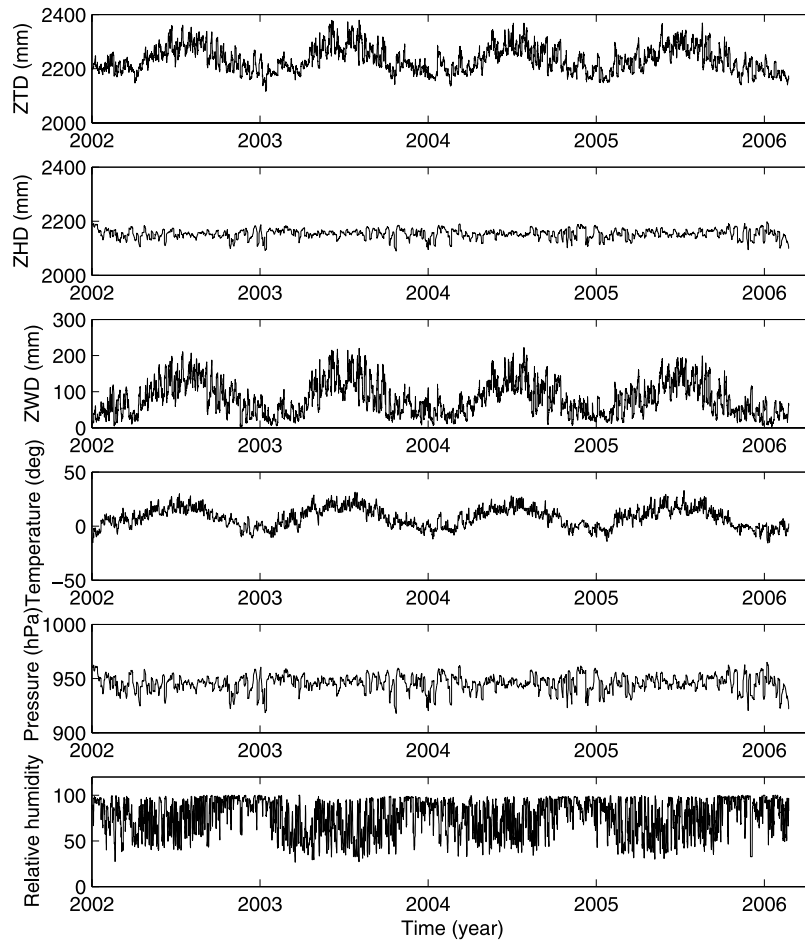


**Figure 4.** Atmospheric parameters at WETT site. From top to bottom are shown zenith tropospheric delay (ZTD), zenith hydrostatic delay (ZHD), zenith wet delay (ZWD), surface temperature, pressure and relative humidity at the site Wettzell (WETT), Germany from the year 2002 to 2006.

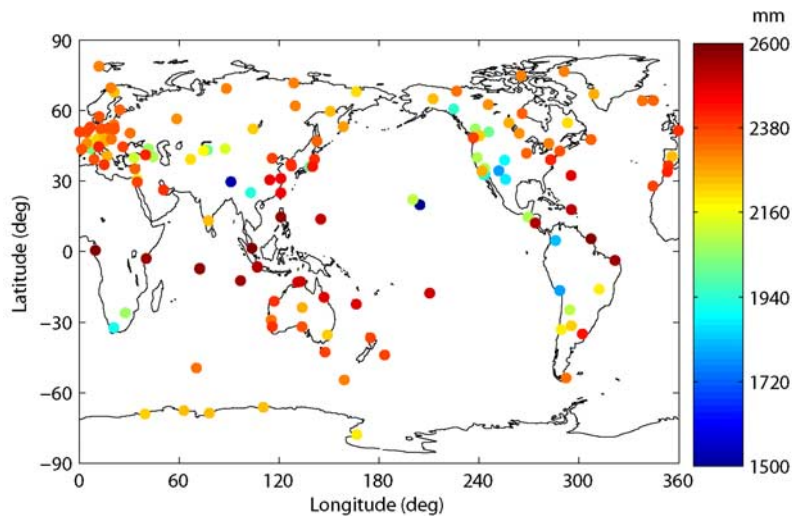


**Figure 5.** Distribution of mean ZTD at global IGS sites.

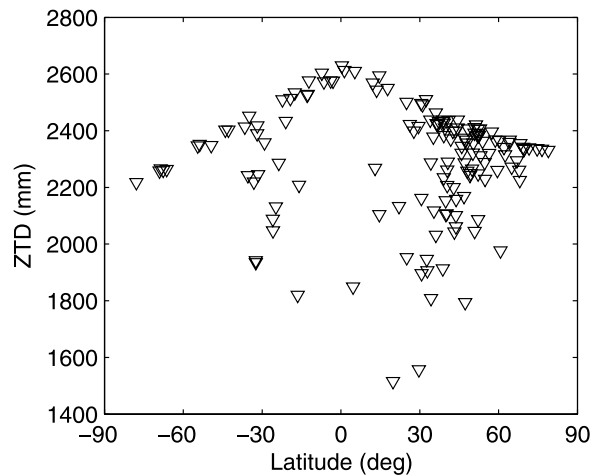


**Figure 6.** Distribution of ZTD with the latitude.

variations of ZTD as well as its possible implications in climate.

## 2. GPS Data and Analysis

### 2.1. GPS Data

[4] The IGS (International GPS Service) was formally established in 1993 by the International Association of Geodesy (IAG) and began routine operations on 1 January 1994 [Beutler *et al.*, 1999]. The IGS has developed a worldwide network of permanent tracking stations with more than 350 GPS sites, and each equipped with a GPS receiver, providing raw GPS orbit and tracking data as a data format called Receiver Independent Exchange (RINEX). Since 1998, the IGS regularly generates a combined tropospheric product in the form of weekly files containing the total zenith tropospheric delays (ZTD) in 2-hour time interval for the IGS tracking stations ([ftp://cddis.gsfc.nasa.gov/gps/products/trop\\_new](ftp://cddis.gsfc.nasa.gov/gps/products/trop_new)). However, the IGS did not provide the ZTD products before 1998, and furthermore, Humphreys *et al.* [2004] demonstrated a drastically attenuated oscillation in the IGS-provided ZTD products between during 1997–2000 and 2000–2004, which was probably caused by the computed ZTD algorithm and network evolution.

[5] Now the fourth Global IGS Data Center in Asian area was established in 2005 at the Korea Astronomy and Space Science Institute (KASI) (<http://gdc.kasi.re.kr>). It archives all available near-real-time global IGS observation data (<ftp://nfs.kasi.re.kr>), including collecting more regional permanent GPS stations data in Asia-Pacific areas. It will contribute to geodesy and atmosphere research activities in a global scale. This study selects the globally distributed 150 IGS sites with better continuous observations spanning more than 4 years (Figure 1), and most sites observations are from 1994 to 2006. The long time span of continuous GPS observations provides important information for the long-term trend and seasonal variation of ZTD.

### 2.2. Zenith Tropospheric Delay Retrieval Process

[6] The quantity observed by the GPS receiver is the interferometric phase measurement of the distance from the GPS satellites to the receiver. The processing software must resolve or model the orbital parameters of the satellites, solve for the transmitter and receiver positions, account for

ionospheric delays, and solve for phase cycle ambiguities and the clock drifts, in addition to solving for the tropospheric delay parameters of interest. This requires the same type of GPS data processing software as that which is used for high precision geodetic measurements. We use the GAMIT software [King and Bock, 1999], which solves for the ZTD and other parameters using a constrained batch least squares inversion procedure. In addition, this study uses the newly recommended strategies [Byun *et al.*, 2005] to calculate ZTD time series with temporal resolution of 2 hours from 1994 to 2006.

[7] The GAMIT software parameterizes ZTD as a stochastic variation from the Saastamoinen model [Saastamoinen, 1973], with piecewise linear interpolation in between solution epochs. GAMIT is very flexible in that it allows a priori constraints of varying degrees of uncertainty. The variation from the hydrostatic delay is constrained to be a Gauss-Markov process with a specified power density of  $2 \text{ cm}/\sqrt{\text{hour}}$ , referred to below as the “zenith tropospheric parameter constraint.” We designed a 12-hour sliding window strategy in order to process the shortest data segment possible without degrading the accuracy of ZTD estimates. The Gauss-Markov process provides an implicit constraint on the ZTD estimate at a given epoch from observations at proceeding and following epochs, which means that the accuracy is expected to be lower at the beginning and end of each window. We therefore extract ZTD estimates from the middle 4 hours of the window and then move the window forward by 4 hours. Finally, the ZTD time series from 1994 to 2006 are obtained at globally distributed 150 IGS sites with temporal resolution of 2 hours. Figure 2 shows the uncertainties for the ZTD solutions at 150 sites as a histogram where the vertical axis is the number of GPS ZTD solutions. It can see that the mean uncertainty of ZTD is about 3 mm.

### 2.3. Analysis Methods

[8] To fit the time series, a model with a linear trend and a seasonal component for ZTD has been used. This model is described by the following function [Feng *et al.*, 1978]:

$$ZTD_t = a + bt + \sum_{k=1}^2 [c_k \sin(2\pi(t - t_0)/p_k + \varphi_k)] + \varepsilon_t \quad (3)$$

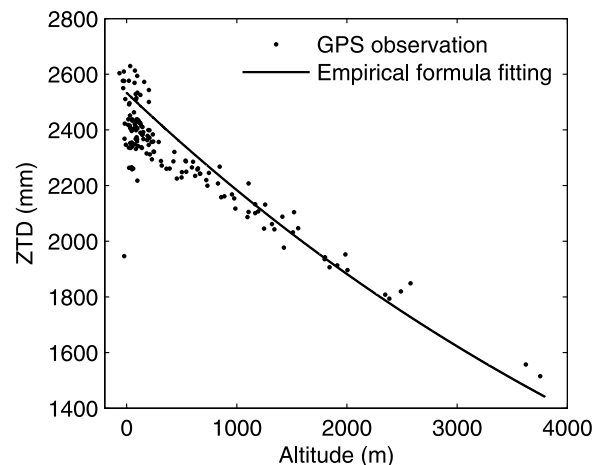


**Figure 7.** Distribution of ZTD with the altitude (above the global mean sea level).

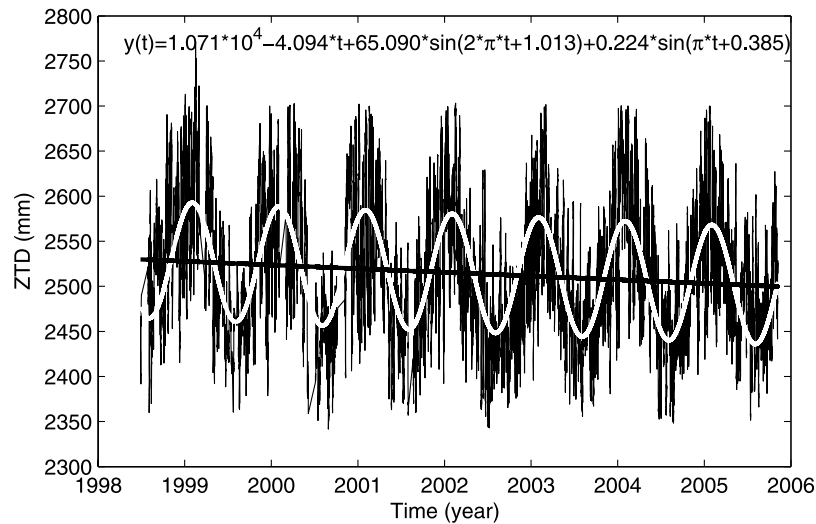


**Figure 8.** ZTD time series at TOW2 station, Australia. The solid line is the fitting results, consisting of a linear decrease and seasonal components.

where  $a$  and  $b$  are the constant and linear terms,  $c_k$ ,  $p_k$ , and  $\varphi_k$  are the amplitude, period, and phase at period  $k$ , respectively, and  $\varepsilon_t$  is the residual. We analyzed all the ZTD time series of each GPS station with Fast Fourier transform and found that the most obvious periods of all GPS stations' ZTD time series are about 359.5 days and 180.1 days. For example, Figure 3 shows the period power chart of ZTD time series at Wuhan (China) GPS site. It has shown clear annual and semiannual variations. No other periods stand out, so we here analyze the ZTD time series using  $p_1 = 1$  year and  $p_2 = 0.5$  year in equation (3). Through the method of least squares we can determine the unknown parameters in equation (3) with

the original series of 2-hour ZTD, and then we further analyze the characteristics of annual and semiannual variations and those of the constant and linear terms.

### 3. Results and Discussions

#### 3.1. Zenith Tropospheric Delay

[9] The ZTD consists of the hydrostatic delay (ZHD) and wet delay (ZWD). The ZHD can be well calculated from surface meteorological data, ranging from 1.5 to 2.6 m, which accounts for 90% ZTD. It derives from the relationship with hydrostatic equilibrium approximation for the atmosphere. Under hydrostatic equilibrium, the change in

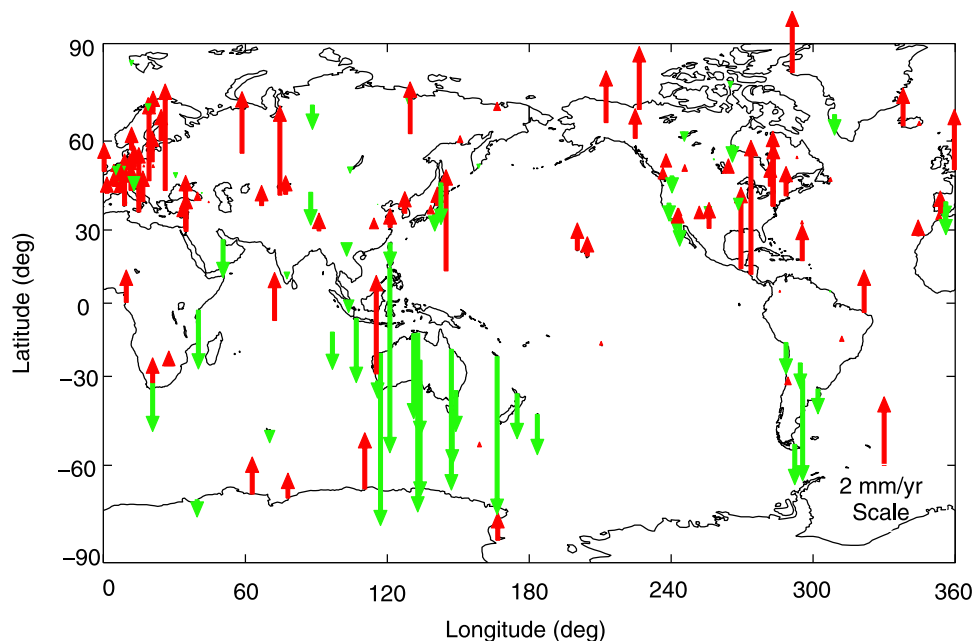


**Figure 9.** Secular variation trend of ZTD at global IGS sites. The red upward arrows represent the increase of secular ZTD variations, and the green downward arrows stand for the decrease of secular ZTD variations.

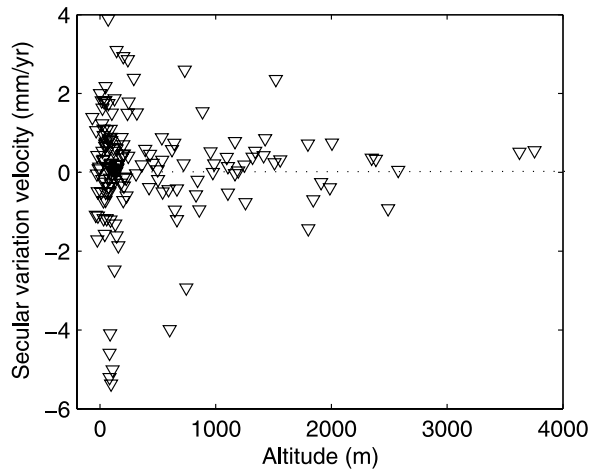


**Figure 10.** Distribution of ZTD secular variation velocities (trend) with the altitude of all IGS sites.

pressure with height is related to total density at the height  $h$  above the mean sea level by

$$dp = -\rho(h)g(h)dh \tag{4}$$

where  $\rho(h)$  and  $g(h)$  are the density and gravity at the height  $h$ . It can be further deduced approximately as

$$ZHD = kp_0 \tag{5}$$

where  $k$  is constant (2.28 mm/hPa) and  $p_0$  is the pressure at height  $h_0$  [Davis et al., 1985]. It shows that the ZHD is proportional to the atmospheric pressure at the site. The ZWD is highly variable due possibly to varying climate, relating to the temperature and water vapor. Unfortunately, only fewer IGS sites have meteorological instruments which can directly obtain the real ZWD or PWV. If one calculated the ZWD or PWV using the meteorological data from the European Centre for Medium-Range Weather Forecasts (ECMWF), it has some differences relative to the real observation results with meteorological instrument data

[Hagemann et al., 2003]. Therefore we here analyze the variation and relationship between atmospheric parameters at GPS stations equipped with the meteorological instruments. For example, the GPS station Wetzell (WETT), Germany has equipped the meteorological instruments. The positions of humidity and temperature sensors are the same as the GPS antenna, and the pressure sensor is 10.5 m below the GPS antenna. The data frequencies of relative humidity, temperature and pressure are all 15 min, and their accuracies are 1.5% (relative to height), 0.3°C and 0.1 mbar, respectively. Figure 4 shows an example of the time series of various atmospheric parameters at the site WETT from the year 2002 to 2006. From top to bottom panels, it sequentially denotes zenith tropospheric delay (ZTD), zenith hydrostatic delay (ZHD), zenith wet delay (ZWD), surface temperature, pressure, and relative humidity. We examine how much of that correlation between surface measurements. It has been noted that the ZHD is highly proportional to the atmospheric pressure at the site and relatively stable, while the ZWD is positively correlated with the temperature and also correlated with the relative humidity. This is due to the combined effects of increasing evaporation and a strong increase in the water vapor saturation pressure. The correlation coefficient between ZWD and surface temperature is 0.81, and the remaining is maybe correlated to the water vapor. The correlation coefficient between ZTD and ZWD is about 0.95, reflecting a good correlation between ZTD and ZWD variations. In addition, we further analyze and compare these parameters at other GPS stations with meteorological data (MATE (Italy), ONSA (Sweden), NYAL (Norway), TSKB (Japan), WES2 (USA), ALGO (USA), FAIR (Alaska, USA), KOKE (Hawaii, USA), and HART (Australia)) and it has shown almost the same correlations with the WETT station. Therefore it has been indicated that the seasonal variations of ZTD are due primarily to the wet component (ZWD), even though the wet delay is only 10% of the total delay (ZTD). In addition, the ZHD is proportional to the atmospheric pressure (equation (5)), while the pressure is mainly related to height (seeing the following equation (6)), and therefore the ZHD is almost constant, again showing

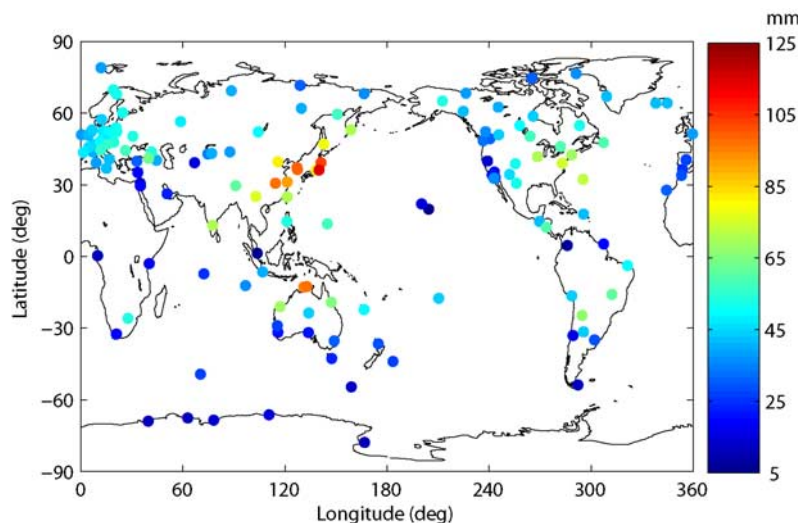


**Figure 11.** Annual variation amplitude of ZTD at globally distributed 150 GPS sites.

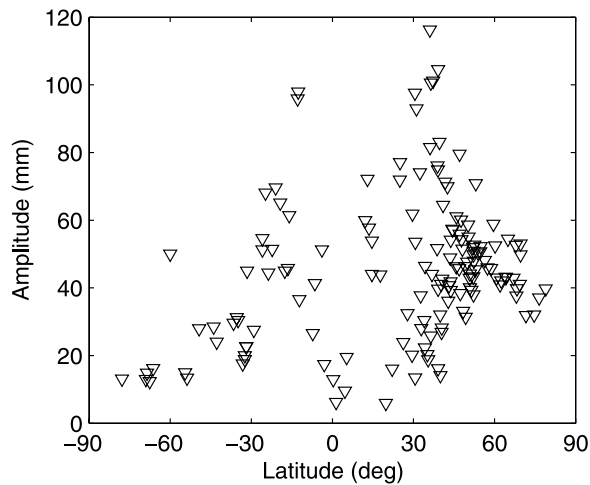


**Figure 12.** Distribution of annual ZTD variation amplitude with the latitude.

that the seasonal variations of ZTD are due primarily to the ZWD.

[10] The mean ZTD values at all GPS sites are shown in Figure 5 as a color map. It has been noted that lower ZTD values are found at the areas of the Tibet (Asia), Andes Mountain (South America), Northeast Pacific and higher latitudes (Antarctica and Arctic), and the higher ZTD values are concentrated at the areas of middle-low latitudes (also see Figure 6). Figure 7 shows the distribution of ZTD at all IGS sites with the altitude (above the global mean sea level). It has been clearly seen that the ZTD values decrease with increasing altitude. This is due to the atmospheric pressure variations with the height increase. Atmospheric pressure is the pressure above any area in the Earth's atmosphere caused by the weight of air. Air masses are affected by the general atmospheric pressure within the mass, creating areas of high pressure (anticyclones) and low pressure (depressions). Low pressure areas have less atmospheric mass above their locations, whereas high pressure areas have more atmospheric mass above their locations. As elevation increases, there are exponentially fewer and fewer air. Therefore atmospheric pressure decreases with increasing altitude at a decreasing rate. The following relationship is a first-order approximation to the height ([http://en.wikipedia.org/wiki/Air\\_pressure](http://en.wikipedia.org/wiki/Air_pressure)):

$$\log_{10} P \approx 5 - \frac{h}{15.5} \quad (6)$$

where  $P$  is the pressure in Pascals and  $h$  is the height in millimeters. On the basis of equation (5), ZHD can be expressed as  $2.28 * 10^{(5-h/15.5)}$ . As the ZHD accounts for 90% of ZTD, we can further deduce the approximate ZTD at all GPS sites as an empirical formula:

$$ZTD = 2.28 * 10^{(5-h/15.5)} / 0.9 \quad (7)$$

where the units of  $ZTD$  and  $h$  are in millimeters, respectively. Comparing GPS-derived ZTD with the empirical formula estimations (Figure 7), it has shown a good consistency.

### 3.2. Trend Analysis

[11] The GPS ZTD time series have been analyzed for 4–12 years at globally distributed 150 GPS sites. Figure 8 shows

an example of an original ZTD time series and the fitting lines at TOW2 station, Australia. The solid line is the fitting results, consisting of a linear decrease and seasonal components (annual and semiannual terms). It has shown a clear trend and seasonal variations of ZTD time series at the TOW2 in Australia with lower values in the winter and higher values in the summer. Using the model from equation (3), the fitting parameters of all GPS site are obtained, including trend and seasonal variation terms. The mean secular ZTD variation trend is about  $1.5 \pm 0.001$  mm/yr. Figure 9 shows the distribution of the secular ZTD variation trends at all GPS sites as the yearly increase or decrease. It can be seen that the trends are positive in most parts of the Northern Hemisphere and negative in most parts of the Southern Hemisphere (excluding positive in Antarctic), corresponding to a systematic increase or decrease of ZTD. It is interesting to note that the downtrend in Australia is larger than other regions. This downtrend of ZTD is probably due to the highly deserted in Australia. In addition, Figure 10 shows the relationship of secular ZTD variation trend with the altitude. It has been seen that the ZTD variation trend decreases with increasing altitude, and furthermore, the ZTD trends are almost symmetrical with altitude. This indicates that the secular ZTD variations are larger at the lower altitude and at the higher altitude the secular ZTD variations hardly increase or decrease. In addition, the sum of downward and upward trends at globally distributed GPS sites is almost zero, which possibly indicates that the secular variation is in balance at a global scale, but subjected to unevenly distributed GPS stations, etc. It need further be confirmed with much denser GPS network in the future. These secular ZTD variation characteristics reflect the total variations of surface atmospheric pressure, temperature and relative humidity, atmospheric vertical motions, etc.

### 3.3. Seasonal Cycle

[12] Meanwhile, the seasonal components are also obtained using equation (3), which can be used to study the seasonal cycle, including amplitude and phase shift. The fitted phase shift is used to determine in which month the seasonal maximum takes place. The annual variation of ZTD ranges from 25 to 75 mm depending on the site, and the

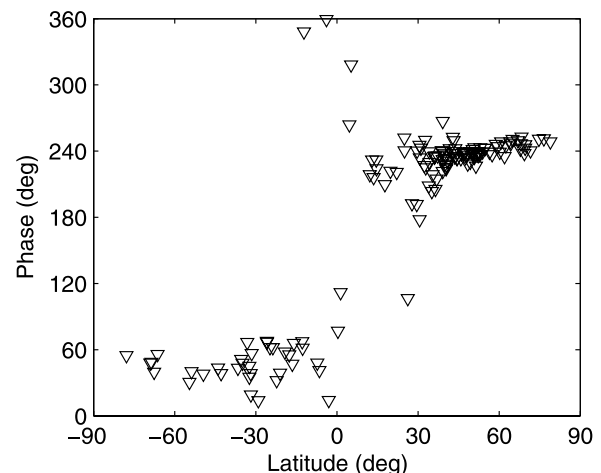


**Figure 13.** Distribution of annual variation phase with the latitude. The phases are counted as clockwise from the north.

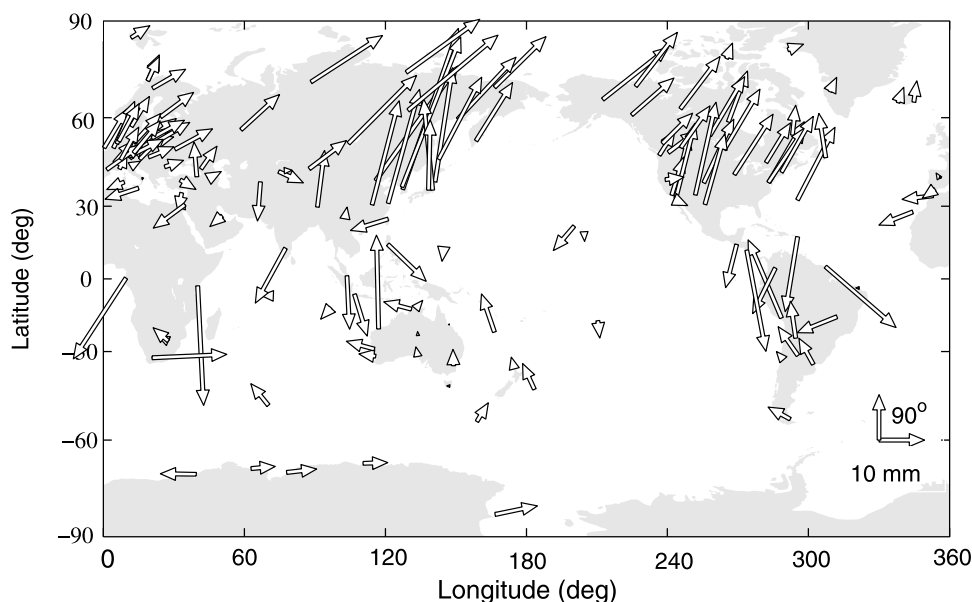


**Figure 14.** Semiannual variation of ZTD at globally distributed 150 GPS sites. The amplitude  $c$  and phase  $\phi$  are defined as  $c \sin(2\pi(t - t_0)/p + \phi)$ , where  $t_0$  is 1995.0 and  $p$  is the period. The arrow lengths stand for the amplitudes. The phases are counted as clockwise from the north.

average amplitude is about 50 mm at most sites (Figure 11). The annual variation amplitudes of ZTD at the IGS sites near oceanic coasts are generally larger than in the continental inland. In addition, larger amplitudes of annual ZTD variation are mostly found at middle-low latitudes (near 20°S and 40°N), and the amplitudes of annual ZTD variation are especially smaller at higher latitudes (e.g., Antarctic and Arctic) and the equator areas (see Figure 12). Sites on the eastern Atlantic and northeast Pacific coasts have lower annual variations, probably because of the moderating effect of the ocean on climate. Sites on the lee side of the Alps have higher annual variation, possibly due to the combined effects of a rain shadow in the winter and high moisture from the Mediterranean in the summer [Haase *et al.*, 2001, 2003; Deblonde *et al.*, 2005]. Figure 13 shows the annual phase distribution with the latitude, where phase values are counted as clockwise from the north. It can be seen that the phase of annual ZTD variation is almost found at about 60° (about February, summer) in the Southern Hemisphere and at about 240° (about August, summer) in the Northern Hemisphere, which is just a half-year difference.

[13] The semiannual variations of ZTD at globally distributed 150 GPS sites are shown in Figure 14. The arrow lengths stand for the amplitudes and the phase values are counted as clockwise from the north. The mean amplitude of semiannual ZTD variations is much smaller than annual variations with about 10 mm. The amplitudes of the semiannual oscillations are much smaller in the Southern Hemisphere than in the Northern Hemisphere. The distribution of the semiannual variation phase with the latitude has no clear symmetry (Figure 15). For example, at the latitudes of 40°N–50°N in the Northern Hemisphere, the semiannual phase is about 30° (about January), while at the latitudes of 40°S–50°S in the Southern Hemisphere, the semiannual phase is about 330° (November).

[14] In addition, we further analyze and compare atmospheric parameters at the GPS stations equipped with meteorological instruments (WETT (Germany), MATE (Italy), ONSA (Sweden), NYAL (Norway), TSKB (Japan), WES2 (USA), ALGO (USA), FAIR (Alaska, USA), KOKE (Hawaii, USA), and HART (Australia)). It has been shown although the ZWD is small accounting for about 10% of the total zenith tropospheric delay (ZTD), the seasonal cycle in ZTD is due primarily to the wet component (ZWD). Furthermore, the seasonal variation phases of ZTD are almost consistent with surface temperature variations with the correlation coefficient of about 0.8. This reflects that annual and semiannual variations of ZTD are due mainly to

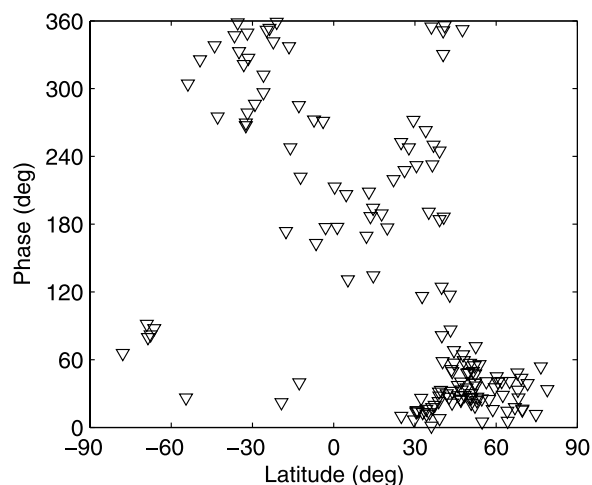


**Figure 15.** Distribution of semiannual variation phase with the latitude. The phase values are counted as clockwise from the north.

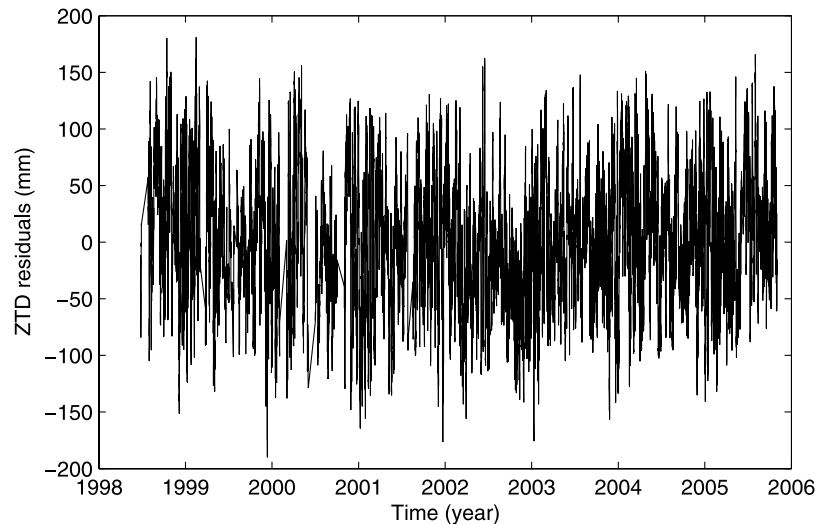


**Figure 16.** ZTD residuals at TOW2 station after removing annual and semiannual terms.

the ZWD variations, about 80% in the surface temperature and 20% mainly in water vapor variations.

**3.4. High-Frequency ZTD Variations**

[15] The unmodeled residuals (observed minus modeled seasonal terms) reflect the high-frequency variation, mainly in ZWD component. For example, Figure 16 shows the ZTD residual at TOW2 station after removing the constant, linear annual and semiannual terms. We estimate the higher-frequency variability by taking the RMS of the ZTD time series after removing the constant, linear annual and semiannual variations as the best-fit sinusoid:

$$RMS = \sqrt{\frac{1}{N} \sum_{t=1}^N (ZTD'_o - ZTD'_M)^2} \quad (8)$$

where  $ZTD'_o$  is the GPS ZTD observation at the time  $t$ ,  $ZTD'_M$  is the best-fit sinusoid modeled value at the time  $t$ , and  $N$  is the total observation number. The RMS of high-

frequency ZTD variations at globally distributed 150 GPS sites is shown in Figure 17. The higher-frequency variability ranges from 15 to 65 mm of delay, once again primarily due to the wet component. The variability depends on ZWD and hence it has a dependence on altitude of the station (Figure 18). Inland stations tend to have lower variability, and ocean and coast stations have higher variability. This is because these stations in particular are located in a region well known for large abrupt changes in the weather, such as Indian, West Pacific, and West Atlantic oceans.

**4. Conclusion**

[16] The GPS signals are delayed due to the effects of dry gas and water vapor when propagating through the neutral atmosphere. The hydrostatic delay is proportional to the surface pressure and the wet delay is a key parameter in atmospheric radiation, hydrological cycle, energy transfer, and the formation of clouds via latent heat. Thereby, the total tropospheric delay (ZTD) is an important parameter of

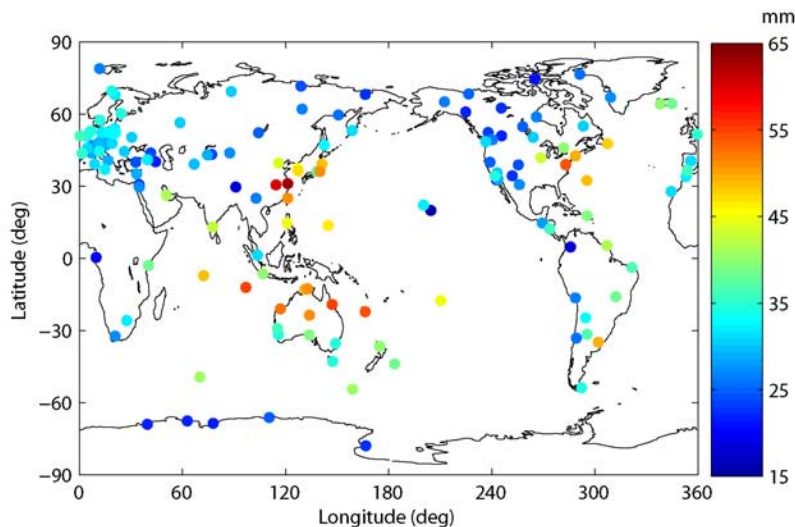


**Figure 17.** RMS of high-frequency ZTD variations at globally distributed 150 GPS sites.

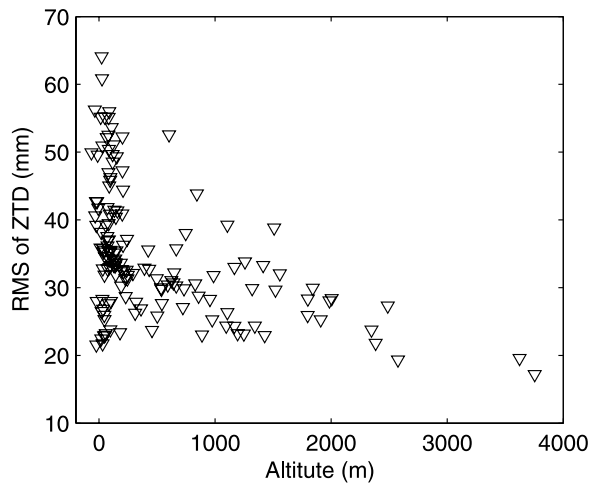


**Figure 18.** Distribution of RMS of high-frequency ZTD variations with the altitude of all IGS sites.

the atmosphere, which directly or indirectly reflects the weather and climate processes, variations, and atmospheric vertical motions, etc. In this paper the ZTD time series (1994–2006) with a resolution of 2 hours at globally distributed 150 IGS sites are obtained and analyzed. Comparing the time series of the zenith tropospheric delay (ZTD), zenith hydrostatic delay (ZHD), zenith wet delay (ZWD), surface temperature, pressure, and relative humidity, it has been noted that the ZHD is highly proportional to the atmospheric pressure at the site and relatively stable and the ZWD is positively correlated with the temperature and also correlated with the relative humidity. The mean correlation coefficient between ZWD and surface temperature is about 0.80 and the correlation coefficient between ZTD and ZWD is about 0.95, reflecting a good agreement between ZTD and ZWD variations. Therefore the seasonal cycles of the ZTD are due primarily to the wet component (ZWD), especially in the surface temperature, even though the wet delay is only 10% of the total delay (ZTD).

[17] The lower mean ZTD values are located at the areas of higher altitude (e.g., the Tibet, Asia, and Andes Mountain in South America) and higher latitude areas (Antarctica and Arctic), and the higher mean ZTD values are concentrated at the areas of middle-low latitudes. The mean ZTD decreases with increasing altitude at an exponentially decreasing rate due to the atmospheric pressure decreasing with the height increasing. The mean secular ZTD variation trend is about  $1.5 \pm 0.001$  mm/yr at all GPS sites. The secular variations are systematically increasing in most parts of the Northern Hemisphere and decreasing in most parts of the Southern Hemisphere (excluding increasing in Antarctic). The ZTD trends are almost symmetrically decreasing with increasing altitude, while the sum of trends at globally distributed GPS sites is almost zero, possibly reflecting that the secular ZTD variation is in balance at a global scale. The annual variation of ZTD ranges from 25 to 75 mm depending on the site, and the mean amplitude is about 50 mm at most sites. The annual variation amplitudes of ZTD at the IGS sites near oceanic coasts are generally larger than in the continental inland. Larger amplitudes of annual ZTD variation are

mostly found at middle-low latitudes (near 20°S and 40°N), and the smaller amplitudes of annual ZTD variation are located at higher latitudes (e.g., Antarctic and Arctic) and the equator areas. The phase of annual ZTD variation is almost about 60° (about February, summer) in the Southern Hemisphere and at about 240° (about August, summer) in the Northern Hemisphere. The mean amplitude of semi-annual ZTD variations is about 10 mm, much smaller than annual variations. The significant semiannual variations with a consistent phase of about 30° (about January) are at above 30°N in the Northern Hemisphere and the amplitudes of semiannual variations in other parts are not significant. In addition, the higher-frequency variability (RMS of the ZTD residuals) ranges from 15 to 65 mm of delay, once again primarily due to the wet component. The variability depends on altitude of the station. Inland stations tend to have lower variability and stations at ocean and coasts have higher variability. This is because these stations in particular are located in a region well known for large abrupt changes in the weather, such as Indian, West Pacific, and West Atlantic oceans.

[18] **Acknowledgments.** Authors thanks referees for so valuable suggestions to greatly improve the paper. We also thank IGS for providing highly precise GPS observations data. This work was supported by the Korea Meteorological Administration Research and Development Program under grant CATER 2006-3104.

## References

- Beutler, G., M. Rothacher, S. Schaer, T. A. Springer, J. Kouba, and R. E. Neilan (1999), The International GPS Service (IGS): An interdisciplinary service in support of Earth Sciences, *Adv. Space Res.*, **23**, 631–635.
- Bevis, M., et al. (1994), GPS meteorology: Mapping zenith wet delays onto precipitable water, *J. Appl. Meteorol.*, **33**, 379–386.
- Byun, S. H., Y. Bar-Sever, and G. Gendt (2005), The new tropospheric product of the International GNSS service, paper presented at 2005 ION GNSS conference, Inst. of Navig., Long Beach, Calif.
- Davis, J. L., T. A. Herring, I. Shapiro, A. Rogers, and G. Elgered (1985), Geodesy by radio interferometry: Effects of atmospheric modeling errors on estimates of baseline length, *Radio Sci.*, **20**, 1593–1607.
- Deblonde, G., et al. (2005), Evaluation of GPS precipitable water over Canada and the IGS network, *J. Appl. Meteorol.*, **44**, 153–166.
- Duan, J., et al. (1996), GPS meteorology: Direct estimation of the absolute value of precipitable water, *J. Appl. Meteorol.*, **35**, 830–838.
- Elgered, G., et al. (1997), Measuring regional atmospheric water vapor using the Swedish Permanent GPS Network, *Geophys. Res. Lett.*, **24**, 2663–2666.
- Emardson, T. R., G. Elgered, and J. M. Johansson (1998), Three months of continuous monitoring of atmospheric water vapor with a network of GPS receivers, *J. Geophys. Res.*, **103**, 1807–1820.
- Fang, P., M. Bevis, Y. Bock, S. Gutman, and D. Wolfe (1998), GPS Meteorology: Reducing systematic errors in geodetic estimates for zenith delay, *Geophys. Res. Lett.*, **25**, 3583–3586.
- Feng, K., J. Zhang, Y. Zhang, Z. Yang, and W. Chao (1978), *The Numerical Calculation Method*, 311 pp., Natl. Def. Industr. Press, Beijing, China.
- Haase, J., H. Vedel, M. Ge, and E. Calais (2001), Radiosonde and GPS Zenith Tropospheric Delay (ZTD) variability in the Mediterranean, *Phys. Chem. Earth A*, **26**, 6–8.
- Haase, J., M. Ge, H. Vedel, and E. Calais (2003), Accuracy and variability of GPS tropospheric delay measurements of water vapor in the western Mediterranean, *J. Appl. Meteorol.*, **42**, 1547–1568.
- Hagemann, S., L. Bengtsson, and G. Gendt (2003), On the determination of atmospheric water vapor from GPS measurements, *J. Geophys. Res.*, **108**(D21), 4678, doi:10.1029/2002JD003235.
- Humphreys, T., M. Kelley, and P. Kintner (2004), GPS-based measurements of atmospheric tides, paper presented at 2004 ION GNSS Conferences, Inst. of Navig., Long Beach, Calif., 21–24 Sept.
- Jin, S. G., and P. H. Park (2005), A new precision improvement of zenith tropospheric delay estimates by GPS, *Current Sci.*, **89**, 997–1000.
- King, R. W., and Y. Bock (1999), Documentation for the GAMIT GPS analysis software, Mass. Inst. of Technol., Cambridge, Mass.

- Manuel, H., et al. (2001), A new strategy for real-time integrated water vapor determination in WADGPS networks, *Geophys. Res. Lett.*, *28*, 3267–3270.
- Niell, A. E. (1996), Global mapping functions for the atmospheric delay at radio wavelengths, *J. Geophys. Res.*, *101*, 3227–3246.
- Rocken, C., R. H. Ware, T. Van Hove, F. Solheim, C. Alber, J. Johnson, and M. G. Bevis (1993), Sensing atmospheric water vapor with the Global Positioning System, *Geophys. Res. Lett.*, *20*, 2631–2634.
- Saastamoinen, J. (1973), Contribution to the theory of atmospheric refraction, *Bull. Geod.*, *107*, 13–34.
- Tregoning, P., R. Boers, and D. O'Brien (1998), Accuracy of absolute precipitable water vapor estimates from GPS observations, *J. Geophys. Res.*, *103*, 701–710.
- Vedel, H., K. S. Mogenssen, and X. Huang (2001), Calculation of zenith delay from meteorological data: Comparison of NWP model, radiosondes and GPS delay, *Phys. Chem. Earth.*, *26*, 497–502.
- Westwater, E. R. (1993), Ground-based microwave remote sensing of meteorological variables, in *Atmospheric Remote Sensing by Microwave Radiometry*, edited by M. A. Janssen, pp. 145–213, John Wiley, Hoboken, N. J.
- 
- J.-H. Cho, J.-U. Park, and P.-H. Park, Space Geodesy Division, Korea Astronomy and Space Science Institute, 61-1 Whaam-dong, Yusong-gu, Daejeon 305-348, South Korea.
- S. G. Jin, Shanghai Astronomical Observatory, Chinese Academy of Sciences, No. 80 Nandan Road, Shanghai 200030, China. (sgjin@kasi.re.kr; sg.jin@yahoo.com)